

Local charging effects in nanocrystalline CdSe filmsD. Toker,¹ I. Balberg,^{1,*} O. Zelaya-Angel,² E. Savir,¹ and O. Millo^{1,†}¹*Racah Institute of Physics and the Center for Nanoscience and Nanotechnology, The Hebrew University of Jerusalem, Jerusalem 91904, Israel*²*Departamento de Física, Centro de Investigación de Estudios Avanzados, P.O. Box 14-740, 07360 Mexico, D.F.*
(Received 31 October 2010; revised manuscript received 14 December 2010; published 15 February 2011)

We performed conductance atomic force microscopy (C-AFM) measurements on nanocrystalline CdSe films prepared by the chemical bath deposition technique. We found a decrease in the local conductance of these films in the vicinity of every spot on the surface to which negative voltage was locally applied via the AFM tip, which we attribute to charging. We found that the currents, measured under such a constant negative bias, decay with time and that the otherwise stable and reproducible positive (tip-bias) currents, measured around the same area, are consequently reduced. This alteration typically extends to a radius of several hundred nanometers around the point of negative-bias application, and it was found to fade on time scales of tens of minutes. We interpret these results as being due to an accumulation of electrons in the vicinity of the tip-sample contact, also yielding nonlinear I - V characteristics for positive tip voltages. This suggests that the electron transport mechanism in these films involves frequent trapping-detrapping events. The comparison with charging phenomena previously reported for various colloidal CdSe nanocrystal arrays indicates that this mechanism is generic to nanocrystalline CdSe systems, independent of structural details and method of preparation.

DOI: [10.1103/PhysRevB.83.085303](https://doi.org/10.1103/PhysRevB.83.085303)

PACS number(s): 73.63.Bd, 68.37.Ps, 72.20.Jv, 72.80.Ey

I. INTRODUCTION

Quantum-dot (or nanocrystalline) solids constitute a new class of advanced materials in which the quantum dots (QDs) are the basic building blocks, analogous to atoms in ordinary solids. Due to the strong size dependence of the electronic properties of single QDs, one would expect to get tunable electronic and optical properties also in QD solids by controlling the size of the QDs composing them and/or their interparticle electrical coupling. The latter depends on parameters such as the interparticle distance, the surface passivation, the phase that surrounds the nanocrystals, and the disorder due to distribution in size and packing geometry. Typically, nanocrystal solids were found to retain a similar size dependence of the optical and electronic properties to that observed for the corresponding single nanocrystals. These include a redshift in the optical absorption and photoluminescence^{1–5} and reduction in the level separations detected via scanning tunneling spectroscopy⁶ with increasing nanocrystal radius.

In our previous work we found that the conductivity of CdSe nanocrystal films prepared using chemical bath deposition increases with the average radius, r , of the nanocrystals comprising the films.⁷ The effect of interparticle distance was investigated for colloidal semiconductor QD solids, where the conductivity was shown to increase^{8,9} and the electronic transitions were found to broaden and to redshift as the average distance was reduced, pointing to a delocalization of the electronic states between the crystallites.^{1,3,6,9–13} However, the transport mechanisms in these materials are still far from being resolved, and despite the large variety of types of QD solids studied so far (or maybe because of that) a general behavior had not yet been identified. In particular, the role played by surface states and deep traps^{1,2,14} in the transport mechanisms has not yet been resolved. In this study we investigate the local conductance of chemically deposited CdSe nanocrystal (NC) films, which constitute disordered QD solids, using conductance atomic force microscopy (C-AFM).

The local nature of the measurement is shown below to induce nonlinear features in the current-voltage (I - V) characteristics for positive AFM-tip bias voltages, as well as charging effects, manifested in a reduction of the local conductance, induced by the application of negative voltages. We interpret these results in terms of intricate trapping-detrapping dynamics that causes bottlenecks for current flow.

II. EXPERIMENTAL

Our CdSe NC films were grown on glass substrates by the chemical bath deposition method, as described in Refs. 4 and 7. The resulting samples consisted of nanocrystals with a size distribution of $\sim 15\%$ with no capping layer (in contrast to the case of colloidal QDs), and were about 200 nm thick. In the present study we measured films with an average nanocrystal radius between 4.4 and 5.7 nm. Since the derivation and the application of the values of these radii have been summarized previously⁵ we just mention them briefly here. The size of the nanocrystallites was determined primarily by x-ray diffraction (XRD)⁴ and further checked by transmission electron microscopy (TEM) and scanning tunneling microscopy (STM).⁷ In particular, we found that these structural results are in accordance with the optical and phototransport spectra when interpreted as associated with the quantum confinement effect.^{4,5} It is to be noted in the present context that the results of the XRD yield the average size of the particles.

Our C-AFM measurements were performed using either a commercial Omicron scanning force microscope operating mainly under ultrahigh vacuum, or a NT-MDT scanning force microscope in ambient or N_2 environments. The use of two different systems was to show that the charging phenomena, and in particular the corresponding trapping dynamics (see below), are not due to surface effects or artifacts. In both cases we applied the constant-force contact mode, using MicroMasch TiPt-coated tips with a force constant of

~0.03 nN and a radius of curvature of less than 40 nm. For conductivity measurements a bias voltage was applied between the conducting tip and a macroscopic electrode deposited on the sample (see the inset to Fig. 1), and thus current maps could be measured along with the topography during each scan.⁷ The bias polarity will be referred to as positive when the C-AFM tip is positively biased with respect to the electrode and vice versa.

The AFM laser in the Omicron system is in the near-infrared (IR) region (~830 nm wavelength), while the NT-MDT system uses a visible red-light laser (632–690 nm wavelength). This is important because in both cases the laser illuminates the sample as well as the cantilever, and we found that the red-light illumination induces photocurrent in our samples. We assume that the near-IR illumination does not induce photocurrent as the energy carried by the IR photons is much smaller than the band gap of CdSe. Indeed, previous works on CdSe NC films^{1,15} have found that absorption and photocurrent were obtained only for above-band-gap illumination (although a sub-band-gap surface photovoltage signal was reported for CdSe QD films).² Furthermore, for samples of small average crystallite radius r we could detect current neither in the dark nor under IR illumination. Photocurrent measurements, particularly with the Omicron system, were obtained by illuminating the tip-sample contact with external lasers of $\lambda \sim 530$ nm and $\lambda \sim 670$ nm, both with an intensity of about 5 mW. The reason for using the NT-MDT system was that it is much easier to operate and thus is suitable for our routine measurements, which do not require UHV or variable temperature. We mention in passing that the NT-MDT system enables the application of our technique¹⁶ by which the dark currents and photocurrents can be measured simultaneously, under exactly the same tip-sample contact parameters (even for a supra-band-gap AFM laser). Note, however, that unless stated otherwise, the results to be presented in the following sections were obtained with the Omicron system.

As described in our previous work, the morphology of our CdSe NC films consists of nanocrystal clusters that are 30–200 nm in size. The individual QDs were not always discerned in the AFM measurements, but this was achieved using STM.⁷ The current maps measured via C-AFM correlate with the topography in that the larger currents are measured on top of these clusters.⁷ To further investigate this correlation, we compared in this work the local I - V characteristics obtained on the different topographic features, mainly on top and between the clusters, and found them to be essentially the same (within an area of a few micrometers), with the difference that the characteristics obtained at the “less conducting” spots (low current regions in the current maps, which can also be a result of local degraded tip-sample contact) were shifted to higher voltages, as happens to be the case also when the conductive coating of the AFM tip wears off. Moreover, the features of the I - V curves measured on these less conducting spots showed the same dependence on parameters, such as the temperature (to be discussed elsewhere), the distance d from the counterelectrode, and external illumination, as for the more conducting spots. This indicates that the lower currents detected in the less conducting regions result from a larger contact resistance and are not due to separate conduction networks as was discovered for different materials such as polycrystalline

CdS (Ref. 17) and metal-insulator composites.¹⁸ Therefore, in our data analysis below we consider only the local I - V curves obtained on top of the clusters (at the more conducting spots) using “fresh” tips. These were found, for each sample, to follow the same behavior as the “statistical” I - V curves (constructed from the peaks in the current-intensity histograms of the current images for different voltages) described in our previous publication.⁷ In all the figures, a bunch of repeated I - V curves will be presented for each measurement in order to depict the degree of reproducibility.

III. RESULTS

Before addressing the local charging effects (the main focus of the paper), which are induced by applying negative tip voltages, we will describe the conductance measurements at positive tip bias, in particular, the shape of the local I - V curves. Figure 1(a) presents typical I - V curves for CdSe NC films of different average nanocrystal radius r , taken under dark

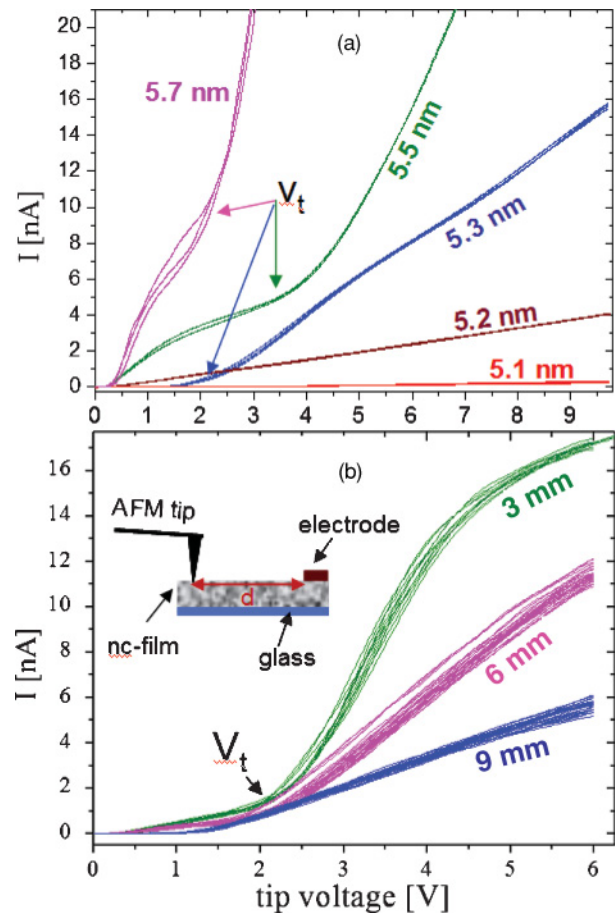


FIG. 1. (Color online) (a) Typical dark I - V characteristics obtained for CdSe NC films of different average nanocrystal radius r , as indicated in the figure. V_t denotes the transition voltage between the low and high differential conductance regimes. (b) The dependence of the I - V curves on the distance d from the counterelectrode, as marked on each set of curves, obtained on a CdSe NC film with $r \sim 5.1$ nm under illumination of the AFM laser in the NT-MDT system. The inset portrays the C-AFM measurement configuration.

conditions (i.e., under illumination of only the AFM near-IR laser), at a distance $d \sim 3$ nm from the counterelectrode. We note in passing that for CdSe NC films with $r < 5.1$ nm only photocurrent (with above-band-gap illumination) could be detected. The strong dependence of the I - V curves on r , both in shape and in current magnitude, is remarkable. For films with $r \leq 5.2$ nm the I - V curves are nearly linear, and with increasing r the I - V characteristics are shown to undergo a transition to a staircaselike shape, in which a distinct crossover from low to high differential conductance regimes is always discerned at a voltage V_t between 1.5 and 3.5 V. It is important to note here that the “macroscopic” I - V measurements (performed using two identical large electrodes deposited on the film) were found to be linear for all the films, with the slope of the curves increasing with r , pointing to the important role played by the “microscopic” tip-sample contact.

Under constant illumination by the supra-band-gap lasers the local conductance was found to increase in such a manner that the I - V curves of each sample resembled the “dark” curves obtained for samples with a larger r . For example, the I - V curves for a NC CdSe film with $r \sim 5.1$ nm, which are linear in the dark, develop, when acquired under illumination, a staircase shape similar to that of the dark I - V curves obtained for the sample with $r \sim 5.3$ nm. The increase in the local conductance after the illumination was turned on reached saturation on a time scale of the order of 100 msec at room temperature. The rise time of the macroscopic photoconductivity was much longer, more than an hour at room temperature and decreasing with temperature. The origin of the difference between these local and macroscopic behaviors is not completely clear at present, but may suggest different charge trapping-detrapping dynamics at the tip environ compared to the bulk. This issue will be further discussed below. Interestingly, the decay of the persistent photocurrent (after the illumination is turned off) was found to be on the order of tens of minutes for *both* the local and macroscopic measurements, reflecting on the trap emptying rate.¹⁹

The dissimilarity between the local (nonlinear) and the macroscopic (linear) I - V scans suggest that the staircase structure observed for large r films results from a local effect. To examine this conjecture we compared local I - V curves taken at different distances d from the counterelectrode. Typical results obtained on a NC CdSe film of $r \sim 5.1$ nm, measured under the illumination of the NT-MDT laser, are shown in Fig. 1(b). Evidently, the curves undergo a transition from a staircase to a linear shape as d increases. We refer to the (maximal) slope of the I - V curves at voltages lower than V_t as the conductance at low voltages, G_L , and to the slope at higher voltages as G_H . Both G_L and G_H were found to decrease with increasing d , but this effect was significantly more pronounced for G_H . In addition, the quality of the tip-sample contact was found to affect V_t and G_L and yet to have only a little effect on G_H . This suggests that V_t and G_L are related to the contact environ, whereas G_H is related to the “bulk” properties. It is important to note that for all samples, V_t was consistently found to be independent of d .

We now discuss the local conductance under negative tip bias and the consequent effect of such measurement on subsequent positive tip-bias measurements. While the positive bias I - V curves taken at similar locations are always

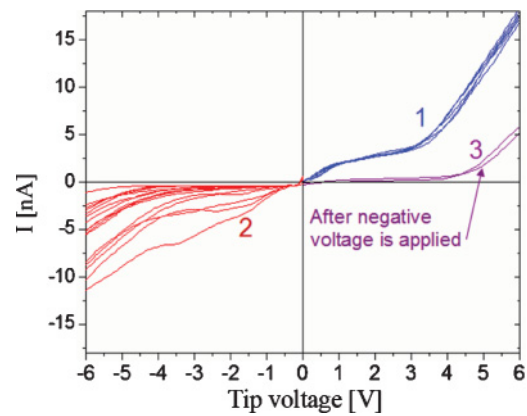


FIG. 2. (Color online) Local I - V curves obtained on the same spot for a CdSe NC film of $r \sim 5.3$ nm. First, a set of only positive tip-bias curves were taken (1), then negative bias curves (2), and finally, positive bias curves were taken again (3), exhibiting reduced currents. Note that the positive bias-voltage curves are quite stable with time, whereas the negative bias curves fluctuate considerably. The characteristics were acquired under dark conditions.

nearly perfectly repeatable, the negative I - V curves alter considerably from one I - V scan to another even when taken at exactly the same spot. The I - V curves shown in Fig. 2 were taken at the same fresh spot, first for positive tip voltages, then for negative voltages, and finally again for positive voltages, as marked on the graph. The negative-voltage I - V curves taken consecutively at the same location were found to fluctuate between successive I - V scans, with a general trend of current reduction with time. As discussed below, under a constant negative voltage the current was found to decrease with time. This behavior of the negative bias was observed regardless of whether positive bias was previously applied to the same location. Furthermore, the positive-voltage I - V curves obtained after acquiring the negative-voltage traces are clearly altered, showing a significantly reduced conductance.

The reduction in the positive-bias conductance as the result of the application of negative voltage to the AFM tip is a local effect. This becomes evident by inspection of Fig. 3, which shows simultaneously acquired topography and current maps for a NC CdSe film with $r \sim 5.3$ nm, under a bias of +0.5 V. Figure 3(a) shows the first topography and current maps, obtained by a continuous scan from the bottom to the top of the image. Figure 3(b) shows the map obtained in a subsequent scan performed in the following way: First, the bottom half of the map was scanned, then the scan was momentarily paused and a negative-bias voltage pulse (-10 V for 65 ms) was applied at approximately the middle point of the last scanned line, indicated by the green dot in the figure. Then, the scan was immediately resumed and the upper half of the map was produced. It is evident that the currents in the vicinity of the affected spot are lowered and the observed effect weakens with the distance from the affected spot. Beyond a radius of $0.5 \mu\text{m}$ the currents remained unaltered. In the subsequent scan [Fig. 3(c)], taken right after the scan in Fig. 3(b) was

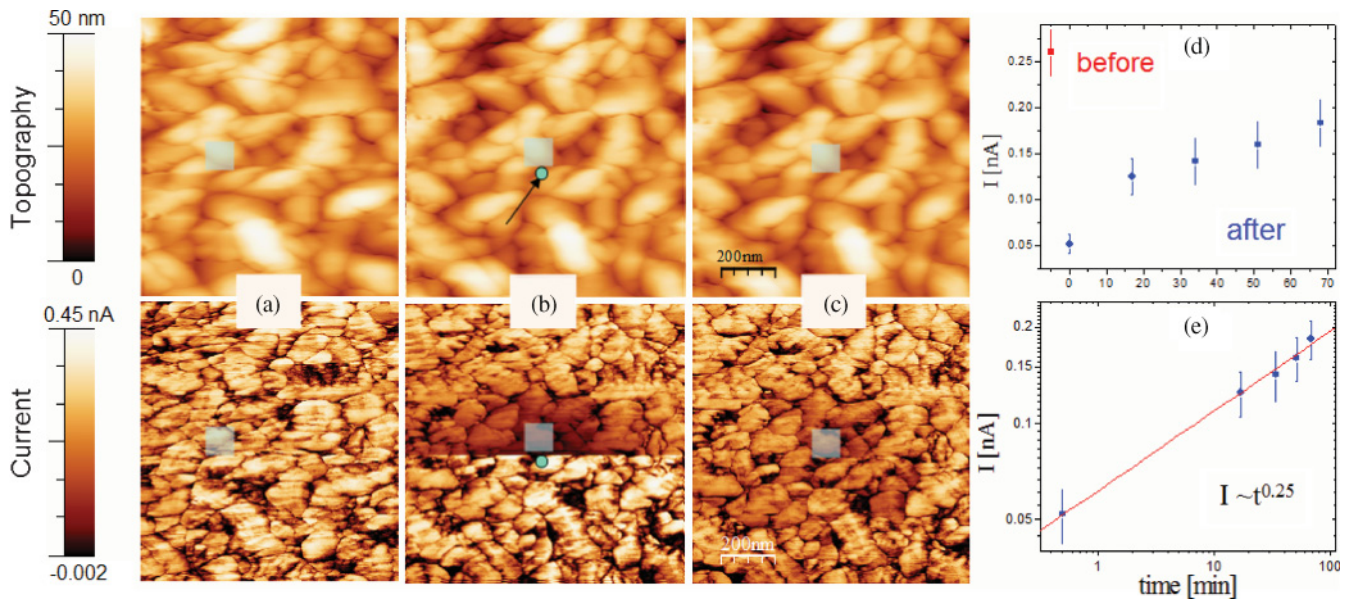


FIG. 3. (Color online) A series of topography (top) and current (bottom) images obtained for the same area on a CdSe NC film with $r \sim 5.3$ nm, under a constant voltage of 0.5 V. The second scan (b) was paused in midway and a short negative-voltage pulse (-10 V for 65 msec) was applied at the position indicated in the figure by the green dot. Immediately afterwards the scan was resumed. The direction of the slow scan is from the bottom to the top of the images. The data in (c) were obtained right after the measurement of (b) had ended. The duration of each of the scans was 17 min. The average current obtained in the same 100 nm^2 area (indicated by the gray square on each image) is plotted as a function of time on linear (d) and log-log (e) scales.

completed, the conductance around the spot appears partially restored. Figure 3(d) shows the average current in an area of $100 \times 100 \text{ nm}^2$ near the affected spot as obtained from the current images in Fig. 3 and from those obtained by further rescanning of the same area. The chosen area is marked on the current images by a gray square. As shown in Fig. 3(d), maps of the same area, obtained after an hour, show that the currents have largely recovered, albeit not completely. We note in passing that the recovery rate appears to conform to a power-law behavior as shown by Fig. 3(e) (but the current range is too small for an unambiguous conclusion). The phenomena described above were observed for all the CdSe NC films studied, but were found to be more pronounced the larger the average radius r of the nanocrystals in the film.

The effect of application of negative tip-bias pulse (-10 V for 65 ms) on the local I - V characteristics and their recovery with time is demonstrated by Fig. 4. In this figure the pristine curves are plotted in black while the curves acquired right after the pulse was applied are drawn in light blue (marked “after charging”). The results clearly manifest a significant current reduction due to this pulse. The healing with time of this effect is also clear from the time evolution of the I - V curves, which show a monotonous current increase with time. To ensure that the I - V curves are obtained in the same location, the sample was repeatedly scanned (at 0 V) and the topography image was used to monitor the drift of the AFM tip and to compensate for it. By this method, I - V measurements could be obtained at the same spot with an error of no more than a few nanometers, even over periods of two hours. Note that even after 120 min only about 60% of the current magnitude is recovered. Long recovery times, such as those observed in Figs. 3 and 4, were observed whenever the negative-voltage-induced charging resulted in a

large modification of the positive I - V curves. When the extent of the charging was small (by using shorter negative pulses and/or lower voltages) a full recovery was observed within less than an hour. Figure 4 also shows that the addition of supra-band-gap illumination further promotes the recovery. The laser was turned on for several seconds after a recovery time of two hours, and the bunch of curves in Fig. 4 marked

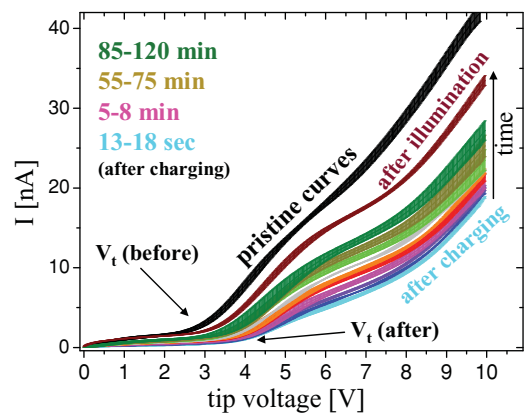


FIG. 4. (Color online) A series of I - V curves obtained on the same spot on a CdSe NC film with $r \sim 5.4$ nm, before (“pristine curves”) and after the application of a negative (tip-bias) voltage of -10 V for 65 msec. I - V curves were measured at the same spot for the next two hours, after which the tip-sample contact area was illuminated ($\lambda = 530$ nm laser) for a few minutes. The (bunch of) dark-red curves (marked “After illumination”) were obtained 20 min after the illumination was turned off.

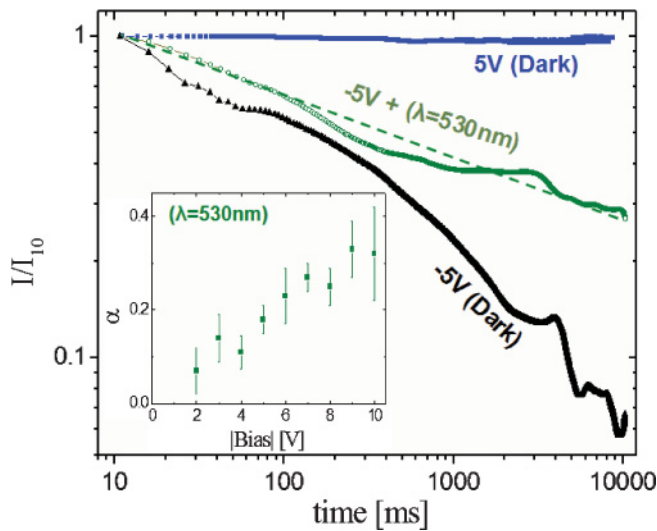


FIG. 5. (Color online) Local $I(t)$ curves (normalized to the current after 10 msec) measured on a CdSe NC film of $r \sim 5.2$ nm at a constant tip voltage of +5 V (blue squares) and -5 V in the dark (black triangles) and under the illumination of a $\lambda = 530$ nm laser (green circles). The inset portrays the slope α as a function of the negative-bias voltage at which the $I(t)$ traces were measured (under illumination). The dashed line is a guide to the eye.

“after illumination” were taken 20 min after the laser was turned off, letting the persistent photocurrent decay.

As noted above, the pristine positive-bias I - V curves were practically stable with time, in contrast to the large fluctuations observed between consecutively acquired negative-bias curves. This is nicely reflected also in the $I(t)$ current-time traces, as depicted by Fig. 5. While the current measured at +5 V hardly changes with time [upper $I(t)$ trace], the $I(t)$ traces measured at -5 V, both in the dark and under illumination, exhibit large fluctuations superimposed on an overall decay with time. The *average* decay rate appears to marginally conform to a power-law behavior, $I(t) \sim t^{-\alpha}$, although the current range may be too small and the traces too noisy for unambiguously establishing such a conclusion. The value of α showed no systematic dependence on bias voltage for $I(t)$ traces measured in the dark, being in the range of 0.3–0.5. Under illumination, however, the slope α was clearly observed to increase with the magnitude of the (negative) bias voltage, as shown in the inset of Fig. 5.

IV. DISCUSSION

The local application of a negative tip voltage was found to reduce the conductance in the vicinity of the spot on the surface to which it was applied, both when measured at a negative or a positive bias. The former, as shown in Fig. 5, is observed as a decrease with time of the negative current measured under a constant bias while the latter is evident when comparing the positive-bias measurements taken before and after the application of the negative bias. From Fig. 3 it is clear that the effect is local since it diminishes with the distance from the affected spot. This observation, and the fact that the current was also found to recover with time (Figs. 3 and 4) rule out a degradation of the conductive coating of the AFM

tip as a possible cause for the decrease in conductance. Since the topography images appear to be unaffected by the process, it is also unlikely that the sample surface was damaged during this process. The recovery with time suggests a mechanism of local charging in the vicinity of the tip-sample contact. It should be noted again that this phenomena was *not* observed for measurements between two macroscopic electrodes.

A decrease in current with time has been reported for CdSe NC films comprising colloidal nanocrystals with $r < 3.1$ nm.^{8,20–23} The current was shown to decay with time as a power law²¹ or as a stretched exponential.²⁰ These phenomena were furthermore similar to the results of our study in that the conductance could be restored with time (after the negative bias is turned off) when the films were kept at room temperature. Furthermore, as in our case, the recovery rate was found to increase following the application of supra-band-gap illumination or, in some cases, with the application of the opposite bias voltage. In each of these works, as well as in other studies of CdSe NC films,^{1,2,24,25} it was concluded that the current is electron (rather than hole) dominated. Von Grunberg further argued that in the case of CdSe the hole states are strongly localized in the nanocrystals while the electrons (having a smaller effective mass) experience smaller barriers and can therefore tunnel out more easily as compared with the holes.²⁵ It was also shown that hole injection may also occur in the films but that the injection barrier for holes is larger than that for electrons.²⁰ The fact that the decrease in the current with time occurs in our case only for negative tip bias also implies a different behavior for electrons and holes at the tip-sample contact, or in the material itself. It was proposed by several groups^{8,21,22} that a large density of charges, composed of trapped electrons, accumulates near the negative electrode. This charge density (in colloidal QD solids) was in fact imaged by Drndic *et al.*²² using electric force microscopy (EFM). Once the negative bias was removed, the excess charge slowly diffused away and the conductance was restored. In our work, the local reduction observed in the positive tip-bias conductance after the application of a negative bias (Figs. 3 and 4) marks the region in which the electrons have accumulated, in analogy to the EFM mapping. In addition, it was found that by using an asymmetric configuration of electrodes such as a gated structure^{21,22} the field near one electrode is made larger than that near the other electrode. It was proposed then that charges are injected only through the former electrode, around which the trapped charge is predominantly accumulated when it is negatively biased.

The fact that in the macroscopic measurement configuration, described in our previous publication,⁷ charging was not observed, may be due to the large area of both electrodes in those measurements (typically a few mm²). In contrast, the electrodes described in Ref. 21, where charging was observed, were about two orders of magnitude smaller, and in our present study the AFM tip-sample contact area was even smaller (less than 50 nm²). It is possible then that when the size of the electrode is large enough the trapping of the electrons is not effective in sufficiently blocking the current since there are too many conduction paths in parallel through which current can flow.

The charging phenomena discovered in the present study and those of others^{8,20–24} were found on NC CdSe films of

a wide range of nanocrystal sizes (from $r \sim 2.2$ nm in the colloidal films to $r \sim 5.7$ nm in the present work) with different types of intergrain connectivity (e.g., with or without capping ligands). This indicates common underlying charging and transport mechanisms. Specifically, it is evident that details such as the passivation of the nanocrystal surface states, surface oxidation (that may take place in our uncapped NC films), and the interparticle distances are irrelevant for the appearance of the phenomenon. This “universality” is remarkable and clearly reflects that important aspects of the charge transport mechanisms are common to all these systems. The observation that only supra-band-gap illumination assists in the current recovery, namely, releases the stored charges, implies that this charge resides predominantly on the nanocrystals (interior or surface states) rather than on the organic capping molecules or on the substrate defect states.²¹ The goal is then to deduce a transport mechanism that would not only account for the above charging phenomena but would also reproduce the nanocrystal-size dependence of the NC film conductivity.

Several physical mechanisms have been proposed to explain the charging phenomena observed for the colloidal CdSe NC films, all assuming that long-range Coulomb interactions play a crucial role because of the high dielectric constant of the nanocrystals [values in the literature are between 6.1–6.2 (Refs. 8 and 25) and 9–9.4 (Refs. 1 and 26)]. Among the explanations are the blocking of charge injection from the contact because of screening of the applied field by the trapped charges²⁰ and a Coulomb glass behavior of the electrons accumulating near the contact.²¹ It was later proposed by Novikov *et al.*²⁴ that the electrical transport in the films involves Lévy statistics of waiting times between charge transmission events.

A distribution of waiting times, with a tail of long sojourn times, would be plausible in the systems under study due to the local fluctuations of the local energy levels of the nanocrystals, which occur also as a result of nearby charge trapping. A long waiting time for charge transport from one nanocrystal to another can also be viewed as a conduction channel being temporarily closed, due to a nearby trapped electron. In our previous work⁷ we proposed that the transport in the system takes place through conduction routes comprising nanocrystals with a relatively small energy mismatch (i.e., with a very small difference in their size). The size dependence of the conductance was attributed there to the fact that in the strong confinement regime (r smaller than the exciton Bohr radius) a small change Δr in the radius r of a nanocrystal results in a more substantial shift in energy levels the smaller the r , thus reducing the effective number of open conduction paths and consequently, to lower conductivity. On top of this quantum-confinement-driven effect, there is a geometrical factor that tends to further reduce the conductance as r decreases. Obviously, the number of intergrain tunnel junctions between the electrodes increases as the average nanocrystal size decreases for any given open conduction path.

Our present C-AFM study provides several additional clues to the understanding of the behavior of these systems, in particular, regarding the positive tip-bias conductance. We suggest that the nonlinearity observed for positive tip-bias I - V curves is due to the same mechanism that leads to the decrease in the current under negative bias. While the flow of holes from

one electrode to the other must be negligible (following the above assumptions that the conductance takes place primarily via electrons) their injection at the tip contact, under positive tip bias, may play a significant role in reducing the buildup of the electron density there. This injection is plausible since the field at the tip contact is larger than at the counterelectrode. The positive-bias current may then have a contribution both from injected holes and from the electrons arriving from the counterelectrode. It is also possible that even in the absence of the hole injection, electrons arriving from the counterelectrode would accumulate in this region more slowly than electrons injected from the tip.

As suggested above, the existence of an electron in a trap state can lead to a temporary decrease in the number of conduction paths in its vicinity. When the number of paths is already limited, as in the case of the small-area tip-sample contact, the conductance is greatly affected, resulting in an effective bottleneck for charge transfer. An electron trapped in such a bottleneck will substantially impede the current as opposed to an electron trapped elsewhere in the sample, in particular, near the counterelectrode that is much larger in size. While the conductance of the bottleneck region depends on the conductivity of the film itself, the flow of charge through it is also restricted by the size of the tip-sample contact area. Therefore, when the bulk conductance of the sample (conductance that would be measured for the same d but with macroscopic electrodes) is smaller than the effective conductance in the bottleneck (e.g., for large enough d and small enough r), the flow of electrons from the counterelectrode under positive tip bias would be small and the accumulation of the electrons in the bottleneck would not occur. The I - V characteristics in such a case will be linear. When the conductance of the sample becomes larger (achieved, for example, by decreasing d), a different steady-state condition is reached. Electrons do accumulate in the bottleneck but their density remains constant with time under the same voltage, because of the injection of holes from the tip. It appears that the interplay between the injection of holes, the flow of electrons arriving from the counterelectrode, and the density of the accumulated charge altogether determine the steady-state current for a specific voltage. The charge accumulated at the bottleneck reduces its conductance, which in turn modifies the voltage division between the bottleneck and the rest of the sample. The process described above concerning the bottleneck enhances the hole injection rate and at the same time reduces the rate of arrival of electrons from the counterelectrode. This, in turn, slows down the accumulation of the electrons until a steady state is obtained. Since positive-bias current transients are very short (typically of the order of 10 msec when the voltage is switched from 0 to 10 V) the charging process must be very short compared with the other processes observed, such as the recovery of the positive conductance after charging.

Following charging, the conductance G_L (and slopes of the staircase structure) and V_t becomes larger. This supports the assumption that the staircase structure results from the accumulation of electrons in the close vicinity of the tip. The charging process causes an increase in the density of the trapped electrons in the bottleneck beyond the density that would have been reached at the steady state for the same initially applied positive-bias voltage. When the charging is

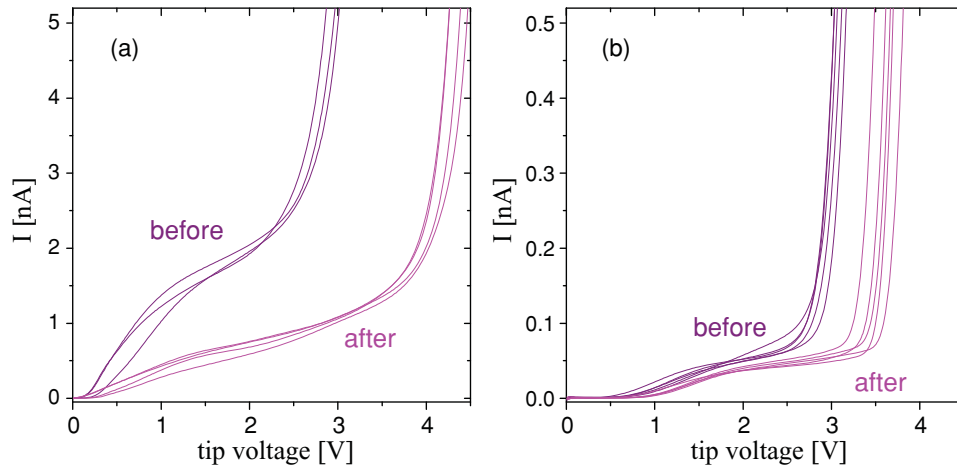


FIG. 6. (Color online) Local dark I - V curves obtained for a NC film of $r \sim 5.7$ nm at 300 K (a) and at 30 K (b) before and after the application of a 0.4 sec pulse of -5 V. The curves were obtained during the same measurement session, using the same tip.

pronounced (as shown in Fig. 3) the region of accumulated electrons extends further into the material (away from the tip contact) and the removal of this excess charge through processes originating at the AFM tip (application of large positive voltages and illumination at the tip-sample contact) is less effective. Supra-band-gap illumination assists the recovery from the charging (Fig. 4 and Ref. 23) and even impedes the charging process itself. The latter effect manifests itself in the smaller decay rate of the current measured at -5 V under illumination compared to the dark (Fig. 5) and also, indirectly, by the fact that under illumination the slope α increases with voltage (inset to Fig. 5), whereas in the dark no such dependence was observed. Illumination increases the density of free charge carriers of both polarities, which may result in a better screening of the trapped electrons, consequently increasing the number of possible conduction routes.

According to our model, the magnitude of the charging effect, and in particular, the extent of the reduction in the positive-bias current, should increase with the amount of charge transferred during the preceding negative-bias application. This leads to two *a priori* counterintuitive results. One, already mentioned above, is that the charging effects become less pronounced as the average QD radius r is reduced and the sample becomes more resistive.¹⁶ This is in contrast to what is typically observed in single-electron tunneling (or charging) experiments, where the Coulomb blockade becomes more significant as the QD becomes smaller. To even further establish our model, we examined the temperature dependence of the charging effects described above. Indeed, while usually the Coulomb blockade smears out as the temperature rises, the behavior observed for the temperature dependence of the charging effects here is just the opposite. This is clearly demonstrated in Fig. 6, where the relative reduction of the positive-bias current (as a result of negative-bias-induced charging) is seen to be stronger at room temperature compared to 30 K, for which the (positive) conductance is significantly reduced.

V. CONCLUSIONS

C-AFM conductance measurements on CdSe QDS were found to reflect not only the bulk conductance of the materials

but also aspects of the local nature of the measurement. The former is manifested mainly in the slope G_H at the high voltage regime of the local I - V curves, which was found to decrease with the distance d from the counterelectrode and increase with the average radius r of the nanocrystals composing the material. The latter parameter was found to induce a staircaselike structure for the local I - V curves when the conductance is large enough. The local effects were explained as resulting from the combination of a transport mechanism for electrons, which is based on trapping in shallow states, and on the microscopic dimensions of the contact between the AFM probe and the material, resulting in a bottleneck for charge-carrier transport near the tip-sample contact. For negative tip voltage the injected electrons restrict the motion of other electrons while proceeding through the bottleneck towards the counterelectrode. As a result, electrons begin to accumulate in the bottleneck, further decreasing its conductance. Under positive tip bias the picture is different since the electrons arrive at the bottleneck from the counterelectrode. When the conductance of the sample is larger than that of the bottleneck, the arriving electrons accumulate in the bottleneck but only up to a voltage-dependent density which does not change with time under a constant voltage, due to injection of holes from the AFM tip. This charge density is responsible for the staircase structure of the I - V characteristics. When the conductance of the sample is smaller than that of the bottleneck no accumulation occurs and the I - V curves are linear. This model also accounts for the reduced current measured under positive bias after the application of a negative tip-bias pulse, as well as the dependencies observed for this current reduction on sample conductance, temperature, and illumination.

ACKNOWLEDGMENTS

This work was supported by the Israel Science Foundation (ISF). I.B. acknowledges the support of the Enrique Berman Chair in Solar Energy Research at the HU and O.M. acknowledges the support of the Harry De Jur Chair of Applied Science at the HU.

*balberg@vms.huji.ac.il

†milode@huji.ac.il

- ¹E. Lifshitz, I. Dag, I. Litvin, G. Hodes, S. Gorer, R. Reisfeld, M. Zelnor, and H. Minti, *Chem. Phys. Lett.* **288**, 188 (1998).
- ²L. Kronik, N. Ashkenasy, M. Leibovitch, E. Fefer, Y. Shapira, S. Gorer, and G. Hodes, *J. Electrochem. Soc.* **145**, 1748 (1998).
- ³O. I. Micic, S. P. Ahrenkiel, and A. J. Nozik, *Appl. Phys. Lett.* **78**, 4022 (2001).
- ⁴A. Rivera-Marquez, M. Rubin Falfan, R. Lozada-Morales, O. Portillo-Moreno, O. Zelaya-Angel, J. Luyo-Alvarado, M. Melendez-Lira, and L. Banos, *Phys. Status Solidi A* **188**, 1059 (2001).
- ⁵I. Balberg, E. Savir, Y. Dover, O. Portillo Moreno, R. Lozada-Morales, and O. Zelaya-Angel, *Phys. Rev. B* **75**, 153301 (2007), and references therein.
- ⁶P. Liljeroth, K. Overgaag, A. Urbieto, B. Grandidier, S. G. Hickey, and D. Vanmaelkelbergh, *Phys. Rev. Lett.* **97**, 096803 (2006).
- ⁷D. Toker, I. Balberg, O. Zelaya-Angel, E. Savir, and O. Millo, *Phys. Rev. B* **73**, 045317 (2006).
- ⁸M. Drndic, M. V. Jarosz, N. Y. Morgan, M. A. Kastner, and M. G. Bawendi, *J. Appl. Phys.* **92**, 7498 (2002).
- ⁹D. Steiner, D. Azulay, A. Aharoni, A. Salant, U. Banin, and O. Millo, *Phys. Rev. B* **80**, 195308 (2009).
- ¹⁰M. V. Artemyev, A. I. Bibik, L. I. Gurinovich, S. V. Gaponenko, H. Jaschinski, and U. Woggon, *Phys. Status Solidi B* **224**, 393 (2001).
- ¹¹M. V. Artemyev, U. Woggon, H. Jaschinski, L. I. Gurinovich, and S. V. Gaponenko, *J. Phys. Chem. B* **104**, 11617 (2000).
- ¹²L. Jdira, K. Overgaag, J. Gerritsen, D. Vanmaelkelbergh, P. Liljeroth, and S. Speller, *Nano Lett.* **8**, 4014 (2008).
- ¹³D. Steiner, A. Aharoni, U. Banin, and O. Millo, *Nano. Lett.* **6**, 2201 (2006).
- ¹⁴E. Lifshitz, I. Dag, I. D. Litvint, and G. Hodes, *J. Phys. Chem. B* **102**, 9245 (1998).
- ¹⁵C. A. Leatherdale, C. R. Kagan, N. Y. Morgan, S. A. Empedocles, M. A. Kastner, and M.G. Bawendi, *Phys. Rev. B* **62**, 2669 (2000).
- ¹⁶D. Azulay, O. Millo, I. Balberg, H. W. Schock, I. Visoly-Fisher, and D. Cahen, *Sol. Energy Mater. Sol. Cells* **91**, 85 (2007).
- ¹⁷D. Azulay, O. Millo, S. Silbert, I. Balberg, and N. Naghavi, *Appl. Phys. Lett.* **86**, 212102 (2005).
- ¹⁸D. Azulay, M. Eylon, O. Eshkenazi, D. Toker, M. Balberg, N. Shimoni, O. Millo, and I. Balberg, *Phys. Rev. Lett.* **90**, 236601 (2003).
- ¹⁹R. H. Bube, *Photoconductivity of Solids* (Wiley, New York, 1960).
- ²⁰D. S. Ginger and N. C. Greenham, *J. Appl. Phys.* **87**, 1361 (2000).
- ²¹N. Y. Morgan, C. A. Leatherdale, M. Drndic, M. V. Jarosz, M. A. Kastner, and M. Bawendi, *Phys. Rev. B* **66**, 075339 (2002).
- ²²M. Drndic, R. Markov, M. V. Jarosz, M. G. Bawendi, M. A. Kastner, N. Markovic, and M. Tinkham, *Appl. Phys. Lett.* **83**, 4008 (2003).
- ²³W. K. Woo, K. T. Shimizu, M. V. Jarosz, R. G. Neuhauser, C. A. Leatherdale, M. A. Rubner, and M. G. Bawendi, *Adv. Mater.* **14**, 1068 (2002).
- ²⁴D. S. Novikov, M. Drndic, L. S. Levitov, M. A. Kastner, M. V. Jarosz, and M. G. Bawendi, *Phys. Rev. B* **72**, 075309 (2005).
- ²⁵H. H. von Grunberg, *Phys. Rev. B* **55**, 2293 (1997).
- ²⁶X. Yang, C. Xu, and N. C. Giles, *J. Appl. Phys.* **104**, 073727 (2008).